Bimetallic Metal-Organic Framework: An Efficient Electrocatalyst for Bromine based Flow Batteries

Raghupandiyan Naresh[a,d], Kalaiarasi Satchidhanandam[c], Kaushek Rahul Ilancheran[c], Bebin Ambrose[b,d], Murugavel Kathiresan[b,d], P. Ragupathy[a,d,*]

[a]Electrochemical Power Sources Division

[b]Electro organic and Materials Electrochemistry Division

[c]Centre for Education (CFE)

CSIR-Central Electrochemical Research Institute, Karaikudi-630003, India

[d]Academy of Scientific and Innovative Research (AcSIR), Ghaziabad-201002, India

Keywords: Metal-Organic Framework, Electrocatalyst, Zinc Bromine, Redox Flow Battery, High Efficiency, High Performance

* To whom all correspondence should be addressed,

E-mail: ragupathyp@cecri.res.in

Tel: +91 04565 241361

1. Experimental section

1.1 Materials

The chemicals used in the present work include zinc bromide ($ZnBr_2$, Alfa Aesar, 99 % purity), Potassium chloride (KCl, Alfa Aesar, 99 % purity), N-Ethyl-N-methylpyrrolidinium bromide (MEP, ICL-Industrial products, 99 % purity), N-Ethyl-N-methylmorpholinium bromide (MEM, ICL-Industrial products, 99 % purity), 1,3,5-benzene tricarboxylic acid (BTC, Alfa Aesar, 98 % purity), 4,4′-bipyridine (Bpy, Alfa Aesar, 98 % purity), $Co(NO_3)_2.6H_2O$ and $Ni(NO_3)_2.6H_2O$ (Alfa Aesar), and dimethylformamide (DMF, Thermo Scientific). The graphite felt GFD 4,6 EA was used as electrodes and it was purchased from SGL Carbon, Germany. The Daramic microporous separator was used in zinc-bromine flow cell study.

1.2 Thermal activation of graphite felt

The graphite felt was annealed at 450 °C for 10 h in a muffle furnace before electrochemical measurements.

1.3 Electrolyte preparation

The electrolyte combination includes 3M $ZnBr_2$ + 3M KCl + 1:1 ratio of MEM (0.89 M) and MEP (0.96 M) dissolved in aqueous medium and served as anolyte (40 mL) and catholyte (40 mL), respectively. The $ZnBr_2$ serve as redox active species, KCl serves as a supporting electrolyte, and ionic liquids such as MEM and MEP serve as bromine capturing agent.

1.4 Synthesis of NiCo-Bpy-BTC

A mixture of 1,3,5-benzene tricarboxylic acid (BTC, 0.525 g, 2.5 mmol), 4,4′-bipyridine (Bpy, 0.390 g, 2.5 mmol), $Co(NO_3)_2.6H_2O$ (0.228 g, 1.25 mmol) and $Ni(NO_3)_2.6H_2O$ (0.363 g, 1.25 mmol) were added to 90 mL of DMF in an autoclave along with a graphite felt (3 cm × 3 cm).

This reaction mixture was maintained at 120 °C for 72 h. After completion of the reaction, the reaction mixture was allowed to cool naturally and filtered. The resultant MOF-anchored graphite felt was washed several with ethanol and DMF to remove the loosely attached molecules/unreacted starting materials and dried at 60 °C for 12 h. The purple-colored solid precipitate of MOF was found on the graphite felt. Finally, the obtained MOF anchored graphite felt was carbonized at 400 °C for 1 h under air atmosphere and the resultant electrode is named as NiCo-MOF@GF.

1.5 Flow cell assembly

The charge-discharge performance was evaluated using the Scribner redox flow cell test system (Model: 857, USA). Two graphite plates with a 6 mm grooved section were used to make the flow cell. A graphite felt with 3 cm × 3 cm was utilized on each side of the graphite plate. Between the graphite plates, a Daramic separator was sandwiched. The electrolyte, which consisted of 40 mL of each anolyte and catholyte having identical composition of 3 M $ZnBr_2$ + 3 M KCl + 1:1 ratio of (0.89 M) MEM and (0.96 M) MEP, was kept separately in a container and pumped into the cell at a flow rate of 30 mL min. The galvanic charge discharge (GCD) analysis was performed at various current densities such as 20, 40, and 60 mA cm^{-2} to charge the flow cell for 15 min and then allowed to discharge up to 0.8 V. The cutoff voltages for the $ZnBr_2$ flow cell are 2.2 V for charging and 0.8 V for discharging, respectively. The high-frequency resistance (HFR) of the device during battery operations is continuously monitored by the Scribner Instrument at a fixed frequency of 10 kHz to probe the internal resistance of the device.

1.6 Physical characterization

The surface morphology of the electrode was investigated through field emission scanning electron microscopy (FESEM) imaging analysis (SUPRA 55VP, Model-Carl Zeiss, Germany) at an

accelerating voltage of 5 kV. The microstructural features of the electrode were investigated by high-resolution transmission electron microscopy (HR-TEM) imaging analysis (Tecnai G2 F20, FEI, Netherland) at an accelerating voltage of 200 kV with a point resolution of 0.24 nm. Further, energy dispersive X-ray analysis (EDAX) was performed to investigate the elemental compositions on the surface of the electrode. To investigate the crystallographic structure of the felts, X-ray diffraction analysis (XRD Brucker D8 ADVANCE) was recorded in the range between 10° to 60° at a scan rate of 3° min^{-1}. The functional groups of the electrode were probed by Fourier transform-infrared spectroscopy (FT-IR, Bruker TENSOR 27, Germany) The surface functionalities of the electrode were examined by X-ray photoelectron spectroscopy (MULTILAB 2000 base system, Thermo Scientific, East Grinstead, UK) using a monochromatic Al Kα X-ray (400 W) with an electron gun spot size of 900 μm. The surface defects of the electrode were analyzed by using Raman spectroscopy (LabRAM HR Evolution) with an oxxius 532 nm and a 50× optical lens was used to obtain Raman spectra. The thermal stability of the electrode was determined by thermogravimetric analysis (TGA, simultaneous TGA-DTA thermal analyzer, NETZSCH STA 44F3 thermal analyzer instrument). The Atomic absorption spectrophotometer (AAS, iCE 3000 Series Thermo Scientific) was used to analyze the cycled catholyte for metallic elements. The standard Ni and Co reference solutions of concentrations in the range between 1-10 ppm were used.

1.7 Electrochemical characterization

The electrochemical activity of the NiCo MOF was investigated by using cyclic voltammetry (CV) and electrochemical impedance spectroscopy (EIS) techniques. For CV and EIS measurements, a three-electrode configuration was utilized with the felts prepared by cutting smaller discs of diameter 6 mm, Ag/AgCl (sat. KCl is used as filling solution), and platinum foil as working,

reference, and counter electrodes, respectively. The electrochemical measurements were carried out in 0.05 M $ZnBr_2$ + 1 M KCl + 300 µL of MEM and MEP at a scan rate of 5 mV s^{-1} under ambient conditions. The electrochemical impedance spectroscopy (EIS) was carried out at an open circuit voltage to probe the electrode solution resistance, and an AC voltage of 10 mV was applied in the frequency range between 1000 kHz to 0.1 Hz.

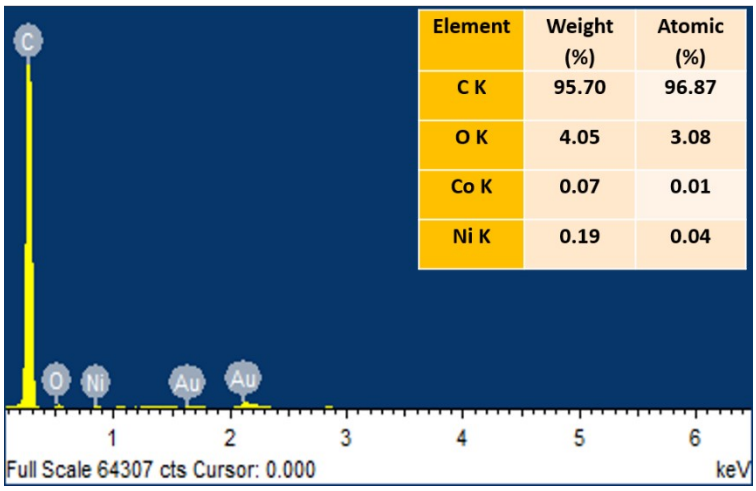

Element	Weight (%)	Atomic (%)
C K	95.70	96.87
O K	4.05	3.08
Co K	0.07	0.01
Ni K	0.19	0.04

Figure S1. EDAX spectra of NiCo-MOF@GF sample obtained from FESEM imaging technique.

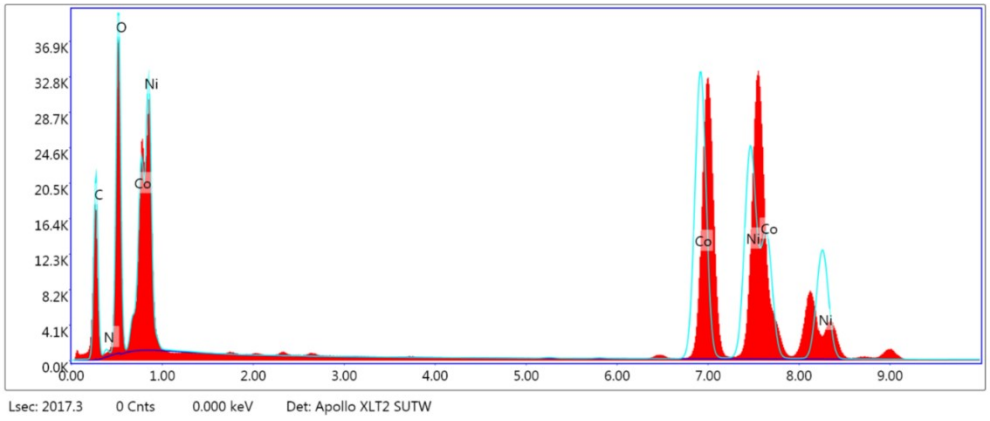

Element	Weight %	Atomic %	Net Int.	Net Error%	KABFactor
C K	7.74	20.74	58.40	0.35	0.8
N K	0.43	0.99	2.00	4.42	1.3
O K	19.15	38.52	121.90	0.28	0.95
CoK	41.24	22.52	248.40	0.15	1
NiK	31.43	17.23	188.20	0.20	1.01

Figure S2. EDAX spectra of NiCo-MOF@GF particle sample obtained from HR-TEM imaging technique.

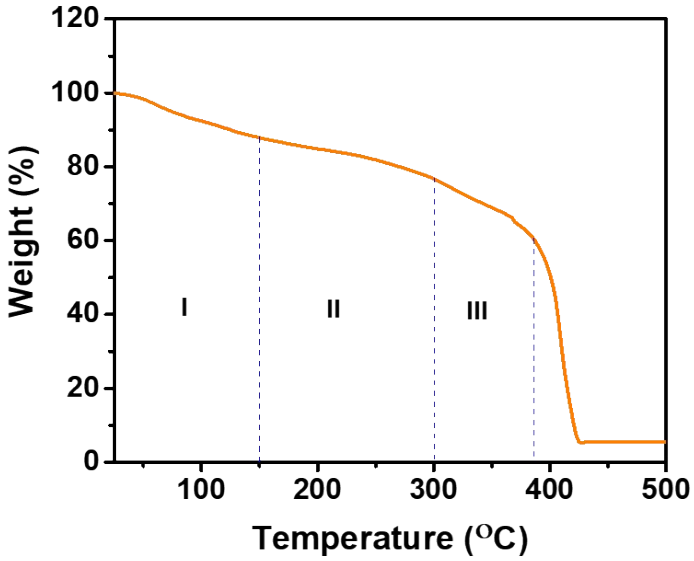

Figure S3. TGA of NiCo-MOF particle sample.

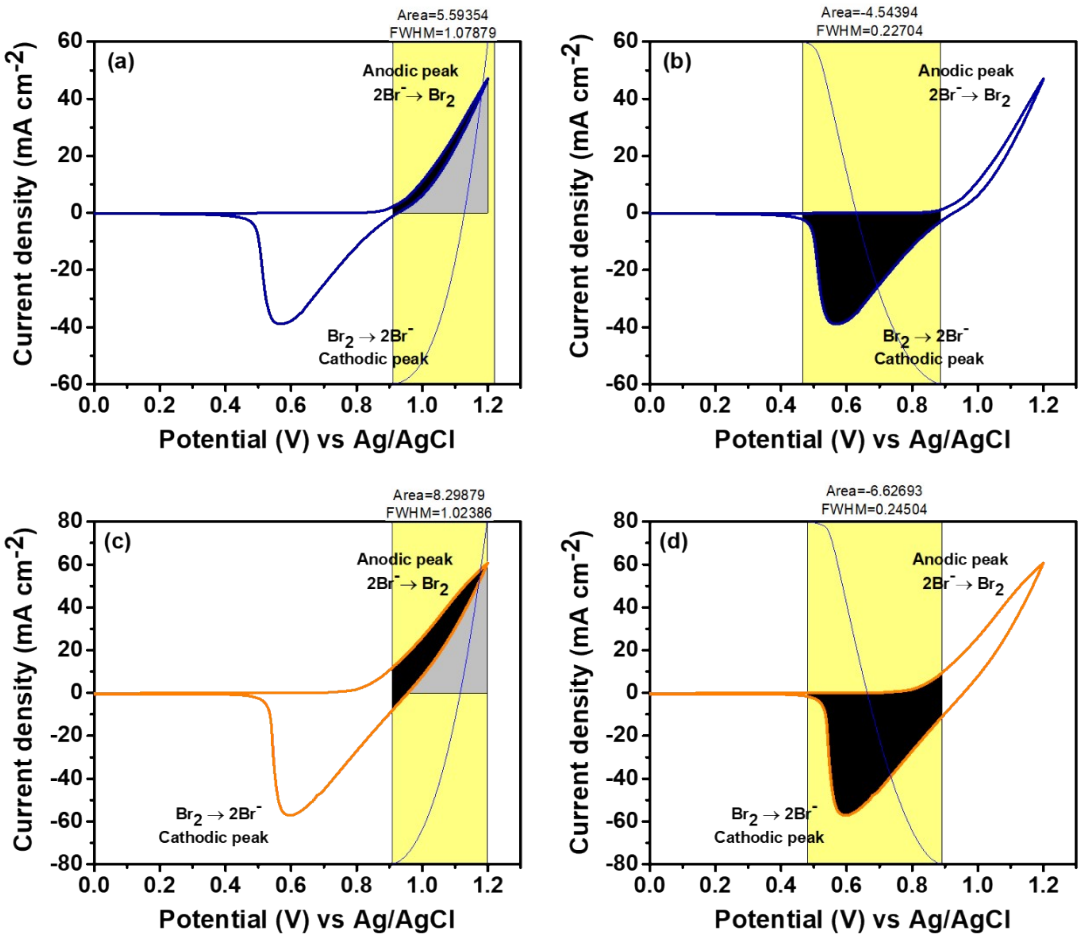

Figure S4. Area under the curve of both anodic and cathodic peaks obtained from cyclic voltammogram measurement (a)-(b) Bare and (c)-(d) NiCo-MOF@GF samples.

From Figure S4, the electrochemically active surface area is much higher for NiCo-MOF@GF (anodic-8.29879 & cathodic-6.62693) than bare (anodic-5.59354 & cathodic-4.54394), as it is beneficial for providing active sites for $2Br^-/Br_2$ redox reaction.

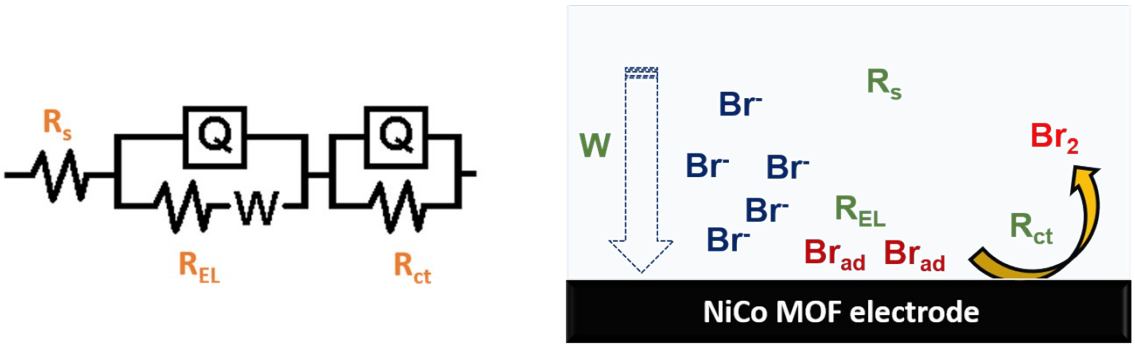

Figure S5. The equivalent circuit model diagram of NiCo-MOF@GF electrode.

Table S1. Electrochemical parameters obtained from electrochemical impedance spectroscopy (EIS) measurement.

S. No.	Electrode	R_{ct} (Ω)	$i_{\circ}$ (mA cm^{-2})	$k_{\circ}$ (cm s^{-1})
01.	Bare	12.10	1.0×10^{-3}	1.0×10^{-7}
02.	NiCo-MOF@GF	1.88	6.8×10^{-3}	7.0×10^{-7}

The exchange current density ($i_{\circ}$) and rate constant ($k_{\circ}$) were calculated from EIS measurements and the corresponding formulas are described below

$$i_{\circ} = RT/nFR_{ct} \text{ …….. (1)}$$

$$k_{\circ} = i_0/nFC_{\circ} \text{ …….. (2)}$$

Whereas R – Gas constant (8.314 J. mol^{-1}. K^{-1})

T – Temperature (K)

n – Number of electrons involved in the redox reaction

F – Faraday's constant (96500 C. mol^{-1})

R_{ct} – Charge transfer resistance (Ω)

$C_{\circ}$ – Concentration of the redox species

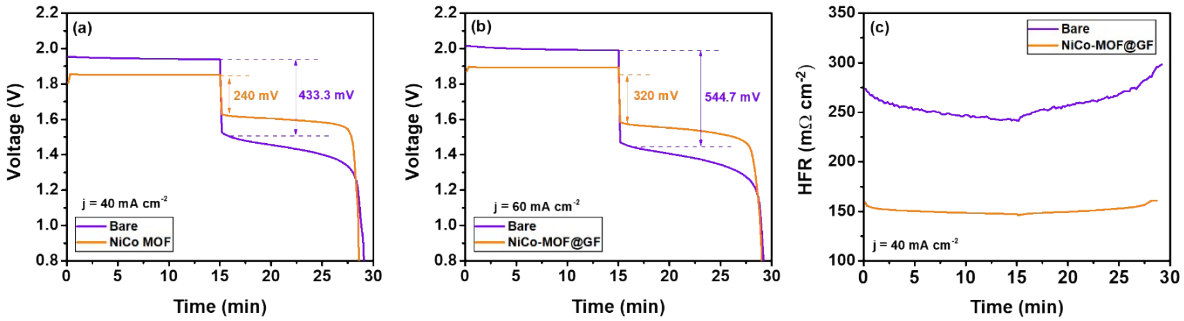

Figure S6. (a)-(b) Galvanic charge discharge profile of bare and NiCo-MOF@GF recorded at 40 and 60 mA cm^{-2} and (c) HFR plot observed at 40 mA cm^{-2}.

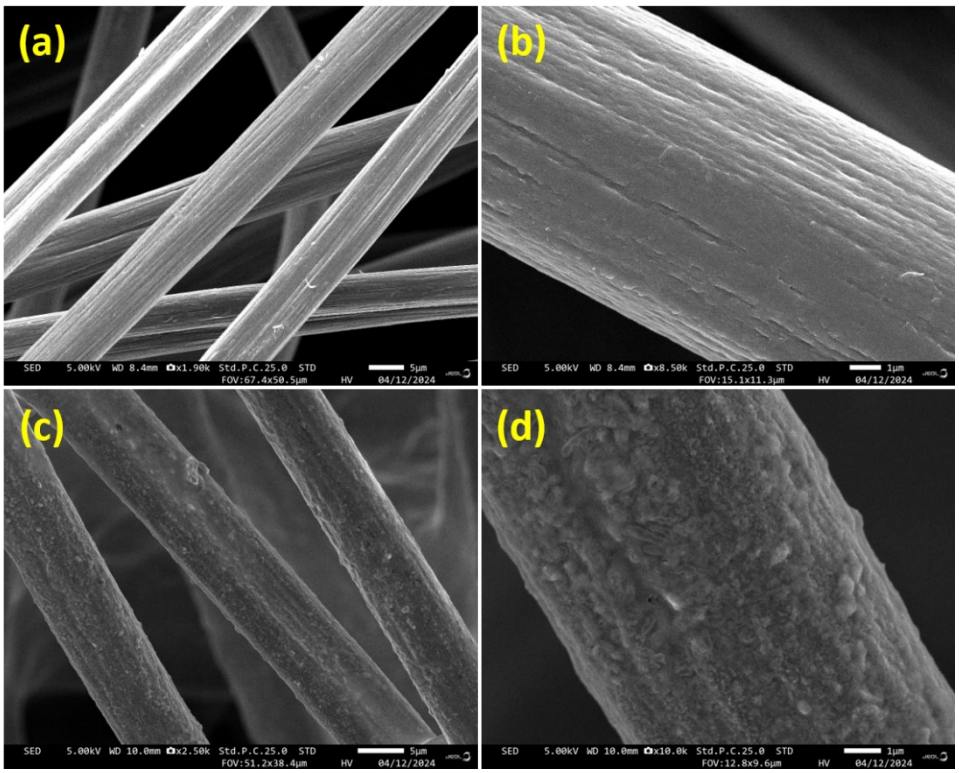

Figure S7. FESEM imaging analysis of samples viewed at different magnifications (a)-(b) Bare and (c)-(d) Post analysis of bare i.e., after ZBRFB measurements.

Table S2. Comparison of electrocatalyst and their ZBRFB performance with the previously reported works.

S. No.	Electrocatalyst	Flow cell performance					Ref.
		Electrolyte	j (mA cm^{-2})	CE (%)	VE (%)	EE (%)	
1.	SWCNT	3M $ZnBr_2$ + 1M $ZnCl_2$ + (1:1 ratio) MEM + MEP	20	82	82.9	70	1
	MWCNT			85	78.3	66.3	
2.	PP/Carbon/CNT composite	2.25M $ZnBr_2$ + 0.5M $ZnCl_2$ + 0.8M MEP	20	-	80.7	73.2	2
3.	Carbonized tubular polypyrrole	2M $ZnBr_2$ + 4M NH_4Cl	40	99	85	83.9	3
4.	Bimodal ordered mesostructured carbon	2M $ZnBr_2$ + 3M KCl + 0.4M MEP	80	96.6	82.9	80.1	4
5.	TiN nanorod array	2M $ZnBr_2$ + 0.4M MEP	160	98	68	66	5
6.	Mesoporous tungsten oxynitride nanofibers	2M $ZnBr_2$ + 4M NH_4Cl + 0.5M $ZnCl_2$ + 0.02M MEP	80	99	81	80	6
7.	Porous nano sheet carbon	2M $ZnBr_2$ + 0.4M MEP	80	98.7	83	82	7
8.	Nitrogen doped carbon felt	2M $ZnBr_2$ + 3M KCl + 0.4M MEP	80	99	83	82.5	8
9.	Activated carbon	3M $ZnBr_2$ + 3M KCl + 1:1M MEM + MEP	30	99	83	82	9
10.	rGO	3M $ZnBr_2$ + 1M $ZnCl_2$ + 1:1M MEM + MEP	20	95	85	80.75	10
11.	Chemically modified carbon paper	3M $ZnBr_2$ + 1M $ZnCl_2$ + 1:1M MEM + MEP	20	95	86	78	11
12.	PtNi@HT-GF	3M $ZnBr_2$ + 1M $ZnCl_2$ + 1:1M MEM + MEP	50	99.9	-	~88	12
13.	NiCo-MOF@GF	3M $ZnBr_2$ + 3M KCl + 1:1M MEM + MEP	60	94.4	78.9	74.5	**Our work**

Table S3. Comparison of voltage drop for various electrocatalysts with the previous reports.

S. No.	Electrocatalyst	Voltage drop (mV)	Current density (mA cm^{-2})	Ref.
01.	SWCNT	320	20	1
	MWCNT	410		
02.	Carbonized tubular polypyrrole	250	40	3
03.	TiN nanorod array	550	160	5
04.	Mesoporous tungsten oxynitride nanofibers	353	80	6
05.	PtNi@GF	276	80	12
06.	**NiCo-MOF@GF**	**82**	**20**	**Our work**
		240	**40**	
		320	**60**	

References

1 Y. Munaiah, S. Suresh, S. Dheenadayalan, V. K. Pillai and P. Ragupathy, *J. Phys. Chem. C*, 2014, **118**, 14795–14804.

2 W. I. Jang, J. W. Lee, Y. M. Baek and O. O. Park, *Macromol. Res.*, 2016, **24**, 276–281.

3 M. C. Wu, T. S. Zhao, R. H. Zhang, L. Wei and H. R. Jiang, *Electrochim. Acta*, 2018, **284**, 569–576.

4 C. Wang, X. Li, X. Xi, W. Zhou, Q. Lai and H. Zhang, *Nano Energy*, 2016, **21**, 217–227.

5 C. Wang, W. Lu, Q. Lai, P. Xu, H. Zhang and X. Li, *Adv. Mater.*, 2019, **31**, 1–8.

6 H. Jung, J. Lee, J. Park, K. Shin, H.-T. Kim and E. Cho, *Small*, 2023, **19**, 2208280.

7 C. Wang, Q. Lai, K. Feng, P. Xu, X. Li and H. Zhang, *Nano Energy*, 2018, **44**, 240–247.

8 W. Lu, P. Xu, S. Shao, T. Li, H. Zhang and X. Li, *Adv. Funct. Mater.*, 2021, **31**, 1–10.

9 R. pandiyan Naresh, K. Mariyappan, K. Selvakumar Archana, S. Suresh, D. Ditty, M. Ulaganathan and P. Ragupathy, *ChemElectroChem*, 2019, **6**, 5688–5697.

10 S. Suresh, M. Ulaganathan and R. Pitchai, *J. Power Sources*, 2019, **438**, 226998.

11 S. Suresh, M. Ulaganathan, R. Aswathy and P. Ragupathy, *ChemElectroChem*, 2018, **5**, 3411–3418.

12 K. Mariyappan, T. Mahalakshmi, T. S. Roshni, P. Ragupathy and M. Ulaganathan, *Adv. Mater. Interfaces*, 2023, **10**, 2202007.